ARMA 11-243

SAND2011-1294C

Coupled Thermal-Hydrological-Mechanical-Chemical Analyses of a Repository in Clay/Shale for High-Level Waste

Stone, C. M.*, Martinez, M. J., Dewers, T., Hansen, F.D, Hardin, E. L., and Argüello, J. G.
*Sandia National Laboratories, Albuquerque, New Mexico, USA; *(Retired)*
Holland, J.F.
Sandia Staffing Alliance, LLC, Albuquerque, New Mexico, USA

This paper was prepared for presentation at the 45th US Rock Mechanics / Geomechanics Symposium held in San Francisco, CA, June 26–29, 2011.

ABSTRACT: This paper describes the modeling efforts undertaken during a recently completed feasibility study of a generic shale repository for disposal of high-level radioactive waste within the United States. A coupled thermal-hydrological-mechanical-chemical analysis of the shale repository was performed using the SIERRA Mechanics code developed at Sandia National Laboratories. Because U.S. efforts have focused on the volcanic tuff site at Yucca Mountain, radioactive waste disposal in U.S. shale formations has not been considered for many years. However, advances in multi-physics computational modeling and research into clay mineralogy continue to improve the scientific basis for assessing nuclear waste repository performance in such formations. Disposal of high-level radioactive waste in suitable shale formations is attractive because the material is essentially impermeable and self-sealing, conditions are chemically reducing, and sorption tends to prevent radionuclide transport. Vertically and laterally extensive shale and clay formations exist in multiple locations in the contiguous 48 states.

1. INTRODUCTION

The results of coupled thermal-hydrologic-mechanical-chemical (THMC) calculations for a generic repository in clay/shale are reported herein. These calculations were a subset of a larger study to assess "Shale Disposal of U.S. High-Level Radioactive Waste" [1]. The problem provided an opportunity to demonstrate the current capabilities of the SIERRA Mechanics software [2] as applied to a repository problem that requires many of the software's unique capabilities. The geometries, material properties, thermal loading, and other features of these calculations were chosen to be representative of potential repository designs.

The development of the SIERRA Mechanics code suite has been funded by the Department of Energy (DOE) Advanced Simulation and Computing (ASC) program for more than ten years. The goal is development of massively parallel multi-physics capabilities to support the Sandia engineering sciences mission. SIERRA Mechanics was designed and developed from its inception to run on the latest, most sophisticated, massively parallel computing hardware. It has the capability to span the hardware range from a single workstation to computer systems with thousands of processors. The foundation of SIERRA Mechanics is the SIERRA toolkit, which provides finite element application-code services such as: (1) mesh and field data management, both parallel and distributed; (2) transfer operators for mapping field variables from one mechanics application to another; (3) a solution controller for code coupling; and (4) included third party libraries (e.g., solver libraries, communications package, etc.).

The SIERRA Mechanics code suite is comprised of application codes that address specific physics regimes. The two SIERRA Mechanics codes that are used for THMC coupling are Aria [3] and Adagio [4]. The physics currently supported by Aria include: the incompressible Navier-Stokes equations, energy transport equation, and species transport equations, as well as generalized scalar, vector, and tensor transport equations. A multi-phase porous flow capability has been recently added to Aria. Aria also has some basic geochemistry functionality available through embedded chemistry packages. The mechanics portion of the THMC coupling is handled by Adagio. It solves for the quasi-static, large deformation, large strain behavior of nonlinear solids in three dimensions. Adagio has some discriminating Sandia-developed technology for solving solid mechanics problems, that involves matrix-free iterative solution algorithms for efficient solution of

extremely large and highly nonlinear problems. This technology is especially suited for scalable implementation on massively parallel computers. The THMC coupling is done through a solution controller within SIERRA Mechanics called Arpeggio.

2. MODELED REPOSITORY GEOMETRIC CONFIGURATION

The repository configuration and heat generation are described in Sections 2.1 and 2.3, respectively, of Ref. 1. They are chosen to represent potential designs but are not meant to specify an actual design. The material properties used in this work also represent relevant geologic materials, but are not site-specific nor based on measured data from any one site.

The model geometry can be defined via a "unit cell" model of a hypothetical waste repository sited in a 600-m thick clay/shale layer overlain by 100 m of sandstone and 200 m of other sediments (Fig. 1). The entire domain is 900 m deep, 63.5 m wide, and 10 m in the horizontal direction perpendicular to the page. The repository is situated 150 m within the clay layer. Repository workings are represented by a horizontal, 5 m diameter access tunnel, with a perpendicular, 0.7 m diameter, 40 m long horizontal emplacement borehole. The waste packages occupy a distance of 30 m from the blind-end of the borehole, followed by a 3 m concrete plug, and finally a 7 m bentonite seal flush with the wall of the access tunnel.

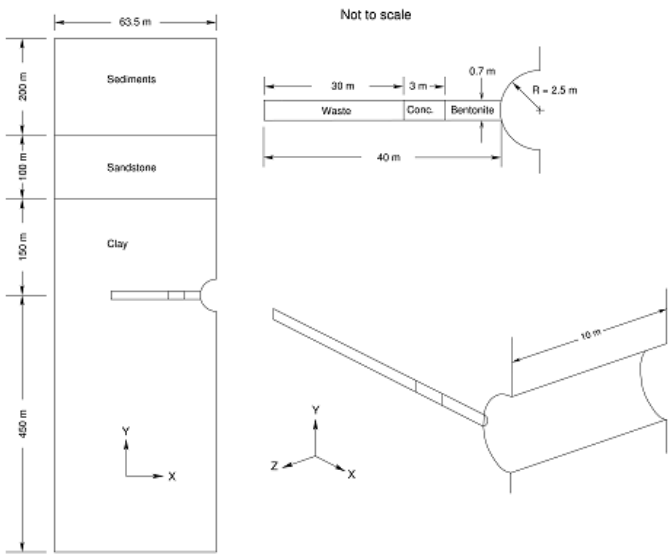

Fig. 1. Multiple View Schematic of the Clay/Shale Repository Model Geometry

The Adagio mechanical analysis and Aria thermo-hydrological-chemical analysis used the same finite element mesh discretization. However, it should be noted that this is not required, as Arpeggio is capable of interpolating information between different meshes and geometries. A detail of the mesh at the repository horizon is shown in Fig. 2. The finite element grid consists of 404,076 nodes and 383,214 eight-node hex elements. The analysis was run on a multi-processor computer using 32 processors requiring approximately five hours of computer time for 10,000 years of simulation time.

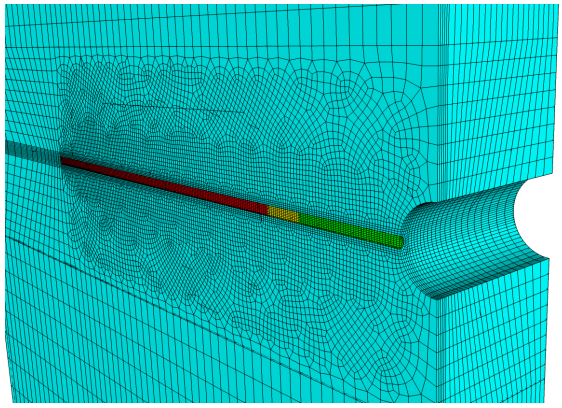

Fig. 2. Finite Element Mesh Detail at the Waste Horizon Showing the Access Tunnel and Horizontal Waste Borehole - the stored waste (red), concrete plug (yellow), and bentonite (green) materials are shown in the borehole.

3. MECHANICAL MODEL DEFINITION

The geometry shown in Figs. 1 and 2 represents a "3D slice" taken from the repository. The vertical planes in the model are symmetry boundaries with normal displacements fixed against horizontal movement. The base of the model is fixed against vertical movement. The geologic materials – clay, sandstone, and sediments – are set to an initial hydrostatic stress condition (the horizontal normal stresses are assumed equal to the vertical overburden stress). The applied external forces are body forces associated with weight of the overburden. Excavation of the access drift and emplacement boreholes is simulated by releasing the initial normal stresses at the free surfaces, over a construction period of one day. After excavation, the thermal loads and water vapor pressures are transferred from Aria and the coupled calculation is run out to 10,000 years. Deformations resulting from the mechanical analysis are transferred to the thermal-hydrologic-chemical problem (THC; forward coupling from the mechanical model to the THC model).

Material property inputs are listed in Tables 1 and 2. With the exception of the clay layer, the stratigraphic materials were modeled as linear elastic. The mechanical properties for the waste canisters, except for the density, are based on the properties of steel. The intent is to have the waste canisters behave as nearly rigid bodies within the clay. The clay materials, the entire clay layer, and the bentonite plug are modeled using the soils and crushable foam material model in Adagio. At present,

Adagio does not have a clay-specific material model in its suite of material models. However, work is currently underway to develop and implement such a model.

Table 1. Physical and Elastic Material Properties

Property	Waste Canister	Concrete Plug	Typical Sandstone	Surf. Sedi-ments
Density (kg/m^3)	1256.7	2247.3	2100	1800
Young's Modulus (GPa)	4.32	23.87	23.0	0.145
Poisson Ratio	0.3	0.2	0.3	0.2
Coeff. of Thermal Expans. ($°C^{-1}$)	11.7×10^{-6}	12.0×10^{-6}	11.6×10^{-6}	11.6×10^{-8}

Table 2. Bentonite and Clay Properties for the Crushable Soil and Foam Model

Property	Bentonite (Backfill/buffer)	Clay Formation
Density (kg/m^3)	1700	2700
Young's Modulus (Pa)	7.00×10^7	7.50×10^9
Poisson Ratio	0.2	0.295
a_0 (Pa)	3.45×10^6	3.45×10^6
a_1	0	0
a_2 (Pa^{-1})	0	0
Cut-off Pressure (Pa)	-2.07×10^6	-2.07×10^6
Coeff. of Thermal Expansion (m/m-C°)	See note	14.0×10^{-6}

Note: Temperature strain function for bentonite (T in Kelvin):
$\varepsilon_T = 3.25E\text{-}06T^2 - 1.18E\text{-}05T - 3.26E\text{-}04 \quad (m/m - K^o)$.

For the soils and crushable foam model in Adagio, the assumed yield surface is a surface of revolution about the hydrostat in principal stress space. In addition, a planar end cap on the normally open end of the surface of revolution is assumed. The yield stress is specified as a polynomial in pressure, p (positive in compression):

$$\sigma_{yd} = a_0 + a_1 p + a_2 p^2 \qquad (1)$$

For this particular analysis, a_0 is non-zero, and a_1 and a_2 are specified to be zero, which results in an elastic-perfectly plastic deviatoric response. This makes the yield surface a cylinder oriented along the hydrostat in principal stress space. The plasticity theories for the volumetric and deviatoric parts of the material response are completely uncoupled. The mean pressure, p, is assumed to be positive in compression, and a yield function is written for the volumetric response as $\phi_p = p - f_p(\varepsilon_v)$ where $f_p(\varepsilon_v)$ defines the volumetric stress-strain curve for the pressure. The deviatoric part of the response is computed using a conventional plasticity theory with radial return to compute the stress at the end of the step.

4. THERMAL-HYDROLOGIC MODEL DEFINITION

The thermal-hydrologic boundary and initial conditions are summarized in Fig. 3. Initially, the entire domain is assumed to be at 20°C and initial saturation corresponding roughly to a (hydrologic) steady state with the upper surface set to 25% liquid saturation.

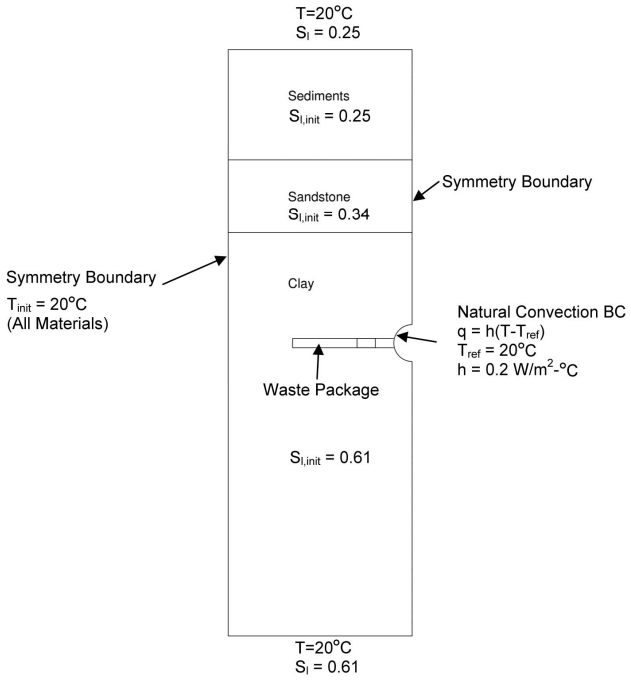

Fig. 3. Schematic of Hydrologic Stratigraphy, Showing Boundary and Initial Conditions

This steady solution was computed separately, and results in nearly uniform saturations in each material,

away from material interfaces. These steady saturations were applied as initial saturations in each material for the heat-driven simulation, with values as depicted in Fig. 3.

The top of the domain represents the ground surface and was set to a temperature of 20°C and a liquid saturation of 25%. The bottom boundary temperature was also set to 20°C. The access tunnel was assumed impermeable to flow and was subject to a natural convection boundary condition with 20°C reference temperature (Fig. 3). All other surfaces were specified as symmetry surfaces, impermeable to mass flow and insulated from heat flow. For the high-level waste glass (HLWG) case, the initial saturation of the host rock was 61%, and this saturation condition was also maintained at the bottom boundary. For the pressurized water reactor (PWR) used nuclear fuel (UNF) cases (discussed below), the initial saturation was increased to 91% to evaluate the potential for pore pressure excursions and the associated mechanical responses.

The thermal-hydrologic model assumes an unsaturated system occupied by water and its vapor. Air is not considered in the present model. The mass balance for water includes pressure-driven flow (including thermally driven flow), gravity, evaporation/condensation, and capillary pressure between liquid and its vapor. The energy equation includes two phase (liquid and gas) mass flow driven convection of sensible and latent heat (evaporation/condensation), heat conduction and buoyancy, and heat generation from the waste package.

The waste package region is a cylindrical domain, assumed to be composed of the clay material, but with uniform volume generation of decay heat. The domain is 0.7 m in diameter and 30 m long (11.5 m^3).

Three different thermal loads, depicted in Fig. 4, are used in the analyses, to represent: (1) fresh HLWG; (2) the hottest PWR UNF considered for the Yucca Mountain license application; and (3) a bounding case for PWR UNF:

- The HLWG thermal power decays with a half-life of about 30 years (representing ^{137}Cs and ^{90}Sr) and rapidly decays to insignificance. For this case the power density for Hanford HLWG was scaled up to represent fresh HLW, such that peak emplacement temperatures approach but do not exceed boiling. This condition was chosen to maximize evaporation and condensation behavior in the near field, without exceeding 100°C.

- The hottest PWR UNF case is based on the average base case PWR UNF thermal output used in performance assessment analyses to support the Yucca Mountain license application, which was then scaled up to envelop the estimated limiting waste stream (ELWS) PWR UNF developed for that application (see Ref. 5, Section 1.3.1.2.5). It thus represents commercial UNF with the greatest thermal decay energy density that was considered for the license application (see Ref. 6, Section 6.1).

The bounding case was developed by scaling up the Yucca Mountain ELWS by approximately 180%, to represent possible hotter, future waste forms. When decay storage is implemented for 50 years prior to emplacement, this bounding case resembles the HLWG case (Fig. 4), hence the THMC analyses were conducted only for the three cases.

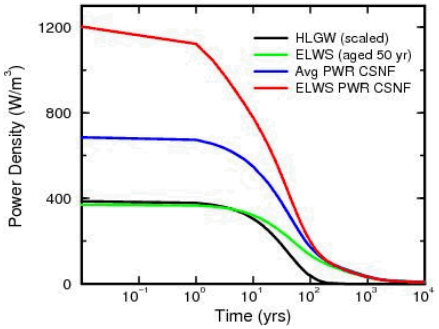

Fig. 4. Power Curves for Waste Used in the Clay/Shale Repository Calculations

Thermal-Hydrologic Material Properties and Flow Models – Material properties and parameters applied in the model are given in Table 3. Again, these values are within a realistic range of values for the type of porous material. Note that the porosity of the clay/shale formation is assigned a large value (30%) to investigate the potential for pore water and vapor mobilization. The permeability of the clay/shale formation is assigned a value of 10^{-16} m^2 for the HLWG case, and 10^{-19} m^2 for the hottest PWR UNF and bounding cases, reflecting a progression of cases intended to explore the maximum range of pore pressure and mechanical responses.

Table 3. Thermal-Hydrologic Material Properties

Property	Clay Formation	Typ. Sandstone	Surf. Sediments	Concrete Plug	Bentonite (Backfill/buffer)
Porosity	0.3	0.2	0.4	0.1	0.276
Permeability (m^2)	10^{-16} to 10^{-19}	10^{-15}	7×10^{-14}	10^{-18}	2.6×10^{-19}
Thermal Diffusivity (m^2/sec)	1.04×10^{-6}	1.40×10^{-6}	1.05×10^{-6}	4.55×10^{-7}	1.00×10^{-6}
VG P_{c0} (kPa)	10	10	8.63	10	10

VG β	1.69	1.69	1.88	1.69	1.69
S_r	0.11	0.11	0.2	0.11[a]	0.11

[a] Residual liquid saturation = 0.005 in relative permeability model.

Curve fits to thermodynamic properties for water (liquid and vapor) are used in the model. The parameters "VG P_{c0}" and "VG β" refer to the van Genuchten model [7]. Capillary pressure, P_c, as a function of liquid saturation, s, was specified as:

$$P_c = P_{c0}\left(s^{-1/\lambda} - 1\right)^{1/\beta}, \quad \lambda = 1 - 1/\beta \tag{2}$$

where the scaled liquid saturation is defined by,

$$s = \left(S_l - S_r\right)/(1 - S_r) \tag{3}$$

and S_l denotes the liquid saturation and S_r the residual liquid saturation.

The Udell cubic function of liquid saturation was used to specify relative permeability for all materials:

$$k_{rl} = s^3$$
$$k_{rg} = (1 - s)^3 \tag{4}$$

5. CHEMICAL MODEL DEFINITION

Boundary conditions for the geochemical model are similar to those used for the thermal-hydrologic model (see Fig. 3). Boundary values of concentration at the top and bottom of the domain are set to zero. Boundary conditions at the sides of the domain are symmetry conditions as described in the previous section. Initially, the entire domain is chosen to have zero concentration, except for the waste package region, which is taken to be equal to unity. The waste package region experiences a radiologic decay rate consistent with first order decay and a half-life of 30.1 years (^{137}Cs), which is also consistent with the thermal loading rate discussed in the previous section. Details and parameter values assumed in the geochemical modeling portion of the study are discussed in Section 7.

6. THERMAL-HYDROLOGIC-MECHANICAL MODEL RESULTS

Mechanical calculations are important for assessing the structural integrity of the access tunnel and waste borehole. The tunnel excavation occurs over several solution steps prior to the start of waste heating. Fig. 5 shows color contour plots of maximum principal stress at the end of the excavation period. The plots show an area of tensile stress that exists in the access tunnel roof and floor at the location of the emplacement borehole. This location is unique due to the intersection of two symmetry planes (x- and z-directions). The constraint of the kinematic boundary conditions on two sides plus the inelastic material response of the clay produces the tensile stress field. This was verified by simulating the excavation sequence using a linear elastic material for the clay. No tensile stresses were observed in the tunnel roof and floor for the linear elastic clay model. This illustrates the need for appropriate, site-specific material models for the clay/shale to get accurate stress results for tunnel integrity assessment. This result also shows the value of three-dimensional calculations and clearly identifies an area for further evaluation.

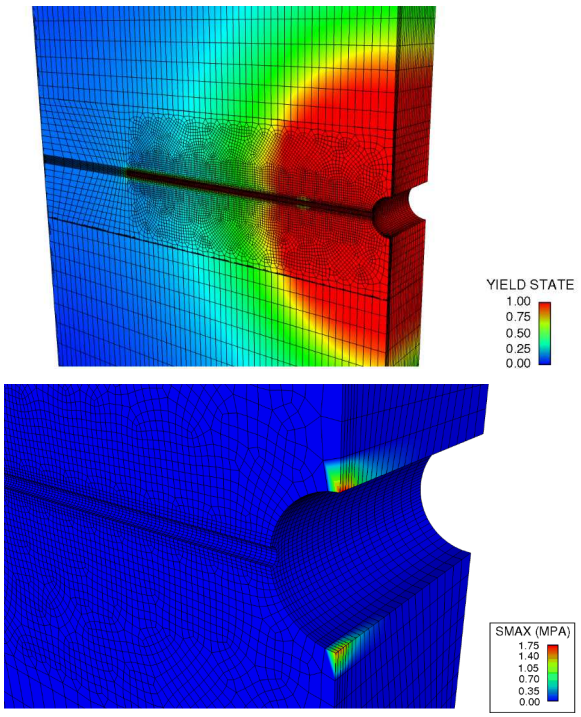

Fig. 5. Color Contour Plots of Post-Processed Yield State Variable and Maximum Principal Stress (SMAX) after Access Tunnel Excavation

Fig. 5 also shows the volume of clay material that is exhibiting nonlinear material response. The plotted yield state quantity is the non-dimensional ratio of the computed von Mises stress divided by the a_0 constant in the constitutive model. If the ratio is less than 1.0, then the material is elastic, and if equal to 1.0, the material is inelastic (stress state is on the yield surface). This figure indicates that the zone of inelastic response extends to a distance of several diameters surrounding the access tunnel, but not the emplacement borehole. The shape and extent of this region, and the relationship between the extent of transient rock disturbance and the permanent excavation disturbed zone (EDZ), depend on the constitutive models used for the clay, and would be subject to further, site-specific investigations.

The peak emplacement borehole temperatures range from 83.5°C for the HLWG case, to greater than 200°C for the bounding case (Figs. 6 and 7). Although the peak

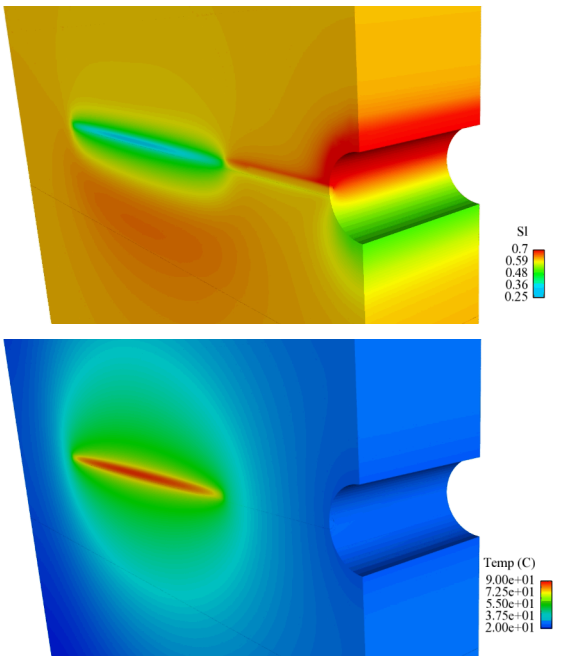

Fig. 6. Liquid Saturation (Sl) and Temperature Distributions near the Waste Packages at 16 Years, for the Fresh HLWG Thermal Case

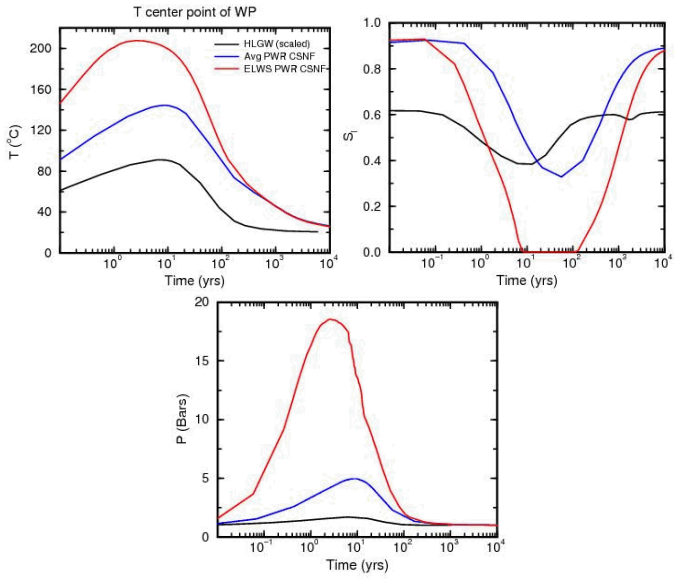

Fig. 7. History of Temperature in the Emplacement Borehole (upper-left); History of Liquid Saturation in the Emplacement Borehole (upper-right); and History of Pore Pressure in the Emplacement Borehole (lower)

temperatures for the PWR cases exceed 100°C, these responses can be readily changed using decay storage as discussed in Ref. 1 (Section 2.3.2). For the HLWG case with relatively small temperature changes, thermal expansion of the solid matrix has a very small effect on the stress state. Also, displacements near the access tunnel are small. From these calculations, the largest structural response of the clay surrounding the access tunnel and emplacement borehole apparently occurs during excavation.

All of the thermal power decay histories are defined such that the repository dries out noticeably within a few years and then re-wets as the repository cools down. For the HLWG case with greater rock permeability (10^{-16} m^2**;** Table 3), water is evaporated near the emplacement borehole, driven away by vapor pressure gradients, and condenses further out, forming a zone of increased saturation. Capillary gradients support liquid flow back toward the borehole. A zone of increased saturation forms below the borehole subsequently seeping downward by gravity and dissipating by capillary action, as shown in Fig. 8. Note that the initial saturation of the host rock was set to 61% for this simulation.

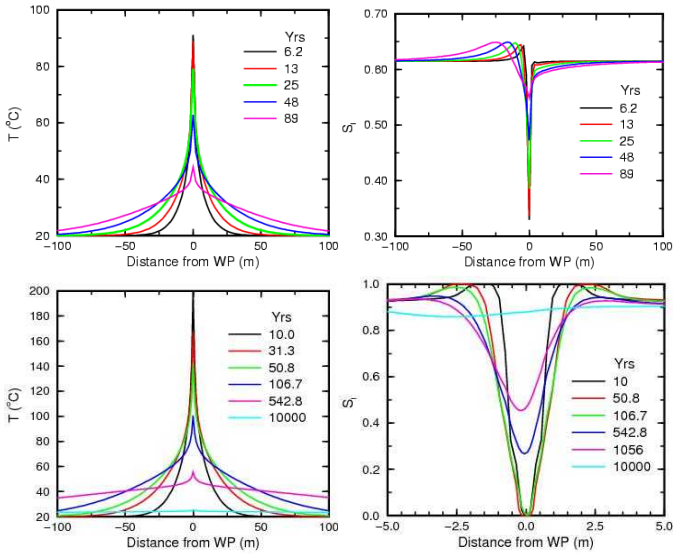

Fig. 8. Temperature (T) and Liquid Saturation (Sl) Distribution as a Function of Vertical Distance from the Waste Package, for the Fresh HLWG Thermal Case (upper) and the Bounding PWR UNF Case (lower)

For the PWR UNF cases with lower permeability (10^{-19} m^2), the dewatering response occurs but the subsequent gravity-driven flow is much weaker, as indicated by the vertical symmetry of saturation profiles (Fig. 8). Notice that the condensate fully saturates the pores, forming a saturated halo about the waste package. Pore pressure response closely follows the vapor pressure of water (Fig. 7), with some dissipation especially for the HLWG case with greater permeability. Note that the initial saturation of the host rock was set to 91% for this simulation.

The spatial extent of elevated pore pressure and the time scale for dissipation are demonstrated for the bounding PWR UNF case, in Fig. 9. Noting that this is a bounding case for which peak temperature greatly exceeds 100°C (see Ref. 1, Section 2.3.2), this result shows that the

duration of elevated temperatures is limited and the thermal gradients in the rock are small beyond a few meters distance. Thermo-diffusion (Soret effect) can therefore be excluded as a significant radionuclide transport process (see Ref. 8, FEP 2.1.11.10.0A).

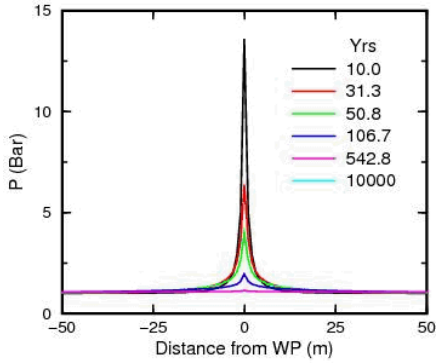

Fig. 9. Pore Pressure Response as a Function of Vertical Distance from the Waste Package, for the Bounding PWR UNF Case

7. GEOCHEMICAL MODELING AND RESULTS

Transport of a single radionuclide is modeled using a simple formulation with first-order radioactive decay and adsorptive retardation, which is part of the present SIERRA Mechanics suite.

Conservation of mass for the *i*th aqueous or gaseous solute mass (c_i is the molar concentration) in a phase π with saturation s and porosity ϕ is given by

$$\frac{\partial}{\partial t}\left(\phi s_{\pi_i} c_i\right) + \vec{\nabla}\cdot\vec{J}_i = \sum_{r=1}^{N_r} \upsilon_{ir} I_r \quad (i = 1,\ldots N) \tag{5}$$

with flux J. The sum on the right hand side is over the total possible N_r homogeneous and heterogeneous reactions I_r in π, where υ_{ir} are the stoichiometric coefficients (number of moles of i participating in the rth reaction). We consider only a single aqueous solute species with concentration c, and account for advective and diffusive flux, so that Eq. (5) becomes

$$\frac{\partial}{\partial t}(\phi s_L c) + \vec{\nabla}\cdot(\vec{v}_L c) = -\vec{\nabla}\cdot(\phi s_L D\vec{\nabla}c) + \phi R \tag{6}$$

Here v_L is the liquid Darcy velocity and D is an effective mass diffusion coefficient which includes a tortuosity, i.e., $D = D_m\tau$. R is the net molar production rate of c, which for our purposes consists of a term accounting for first-order radioactive decay and a term accounting for sorption. Following the treatment of Schwartz and Zhang (Ref. 9, Equation 23.12), Eq. (6) then becomes

$$\frac{\partial}{\partial t}(\phi s_L c) + \vec{\nabla}\cdot(\vec{v}_L c) + \frac{\partial}{\partial t}(s a_m) = -\vec{\nabla}\cdot(\phi s_L D\vec{\nabla}c) + r \tag{7}$$

where the third term on the left-hand-side is the time rate of change of the product of an areal molar concentration s and the specific surface area of mineral per unit bulk volume, a_m, and r accounts for any other chemical reaction rate. When sorption reaction rates are considered rapid relative to transport rates, s will reflect a local equilibrium with the local bulk fluid concentration c, and thus can be represented by a sorption isotherm. Assuming a simple linear isotherm (linear relation between c and s) permits the introduction of a retardation factor R_f in Eq. (7) such that

$$\frac{\partial}{\partial t}(\phi s_L c R_f) + \vec{\nabla}\cdot(\vec{v}_L c) = -\vec{\nabla}\cdot(\phi s_L D\vec{\nabla}c) + r \tag{8}$$

where $R_f = 1 + a_m k/\phi s_L$ with k the isotherm constant. Usually retardation is defined in terms of an apparent distribution coefficient (as a means of relating sorption behavior to experimental measurement) k_d, which relates the total contaminant mass adsorbed per total solid mass to the bulk aqueous concentration. With $k_d = a_m k/\rho_b$ and ρ_b the bulk mass density, $R_f = 1 + \rho_b k_d/\phi s_L$ (Equation 23.14 of Ref. 9, here modified for partially saturated media).

For a solute species undergoing first-order radioactive decay, $r = -\phi s_L R_f \lambda c$, where λ is the decay constant, related to radionuclide half-life by $t_{1/2} = ln(2)/\lambda$ (Ref. 9, Equation 23.16).

Solution in Aria – To solve Eq. (8) for relevant boundary and initial conditions, and to include this in a multi-physics treatment that couples solute transport with multi-phase flow and mechanics, we use Aria. At the time the analysis was performed, the solute reaction and transport solver within Aria required a constant porosity and saturation, and for our problem, a constant retardation factor. With these assumptions, and further assuming a constant D, and with λ and R_f so defined as in the previous section, Eq. (8) becomes

$$\frac{\partial c}{\partial t} - \frac{1}{R_f\theta}\vec{\nabla}\cdot(\vec{v}_L c) = \frac{D}{R_f\theta}\nabla^2 c - \lambda c \tag{9}$$

where the liquid moisture content $\theta = \phi s_L$. This is a form readily solved by Aria.

Parameters – Solving Eq. (9) requires values for the four parameters R_f, θ, D, and λ, which in turn requires estimations for the distribution coefficient k_d, the mass diffusion coefficient D_m, tortuosity τ, half-life $t_{1/2}$, bulk density ρ_b, porosity ϕ, and liquid saturation s_L. These would be considered average values over the spatial and temporal simulation domains. Considering the case of

reaction and transport of ^{137}Cs (chosen for its short half-life to readily permit examination of the predictions of sorption and decay) in a clay-bearing country rock, reasonable values for these parameters are:

k_d = 320 mL/mg (consistent with the range from Table 2)
$D_m = 1.64 \times 10^{-9}$ m^2/sec
$t_{1/2}$ = 30 years (representing ^{90}Sr or ^{137}Cs)
ρ_b = 2.22 g/cm^3
θ = .05 and τ = 0.5 (estimates)

These values yield $(R_f\theta)^{-1} = 0.0014$; $D/R_f\theta = 1.15 \times 10^{-12}$ m^2/sec; and $\lambda = 7.32 \times 10^{-10}$ sec^{-1}.

Results – Because of the short half-life and relatively large retardation factor used in this calculation, transport distances from the waste package are short relative to decay times. This is evident in Fig. 10, which plots a normalized or scaled concentration as a function of time. Initially, the scaled concentration is unity inside the waste package region (see Fig. 3). Parameter values are such that, for ^{137}Cs, a concentration of unity would be about 10^4 mg/L. After 5 years the concentration profile shows a very small migration, on the order of centimeters. Twenty years out, the concentration profile begins to narrow at the center, associated with radioactive decay but also with the relatively larger liquid advective velocity (because of the larger spatial gradients in liquid saturation and heat in this region, during this time). By approximately 30 years, sufficient radioactive decay has led to the near disappearance of solute in this region, and by 60 years (not shown), the solute has nearly disappeared from the solution. This shows that fission products comprising the constituents of HLW that have the greatest specific activities and shortest half-lives are completely isolated from the geosphere overlying the simulated clay/shale repository.

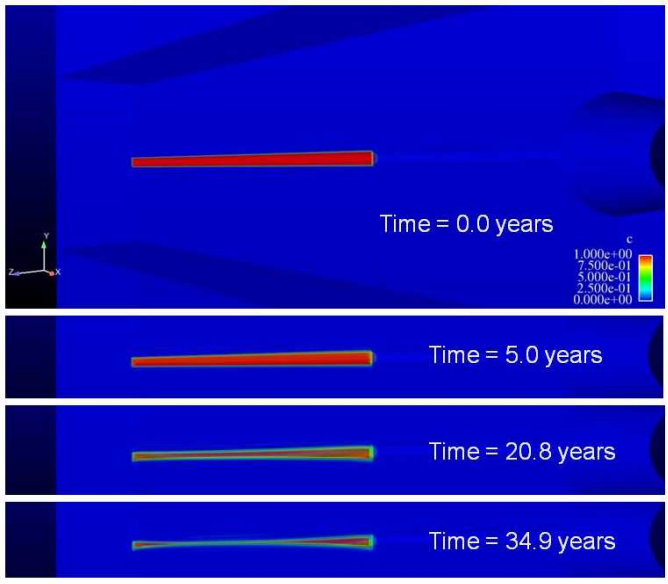

Fig. 10. Normalized or Scaled Concentration of ^{137}Cs near the Waste as a Function of Time

8. MULTIPHYSICS MODELING SUMMARY

Results presented in the foregoing sections are generally consistent with calculations performed by international programs, particularly ANDRA and NAGRA, and discussed in Ref. 1, Section 2.3. The calculations confirm the result presented in that section, that the maximum host rock temperature can be limited by selection or decay storage of waste forms. The duration of elevated host rock temperatures would be limited to a few hundred years, during which substantial dewatering of the near-field host rock could occur, given sufficient permeability. The region of plastic deformation and stress conditions modified by excavation could be dominated by the larger diameter access drift. The extent of the EDZ would be sensitive to site-specific rock constitutive behavior, but the results from these generic simulations are consistent with a maximum extent of a few meters. The behavior of ^{137}Cs in radionuclide transport simulations represents the isolation, and attenuation by radioactive decay, that is expected for disposal in clay/shale formations. Based on these results, and EDZ investigations by international programs (Ref. 1, Section 2.3.1), the extent of the EDZ is limited to a few meters and can be ignored as a transport path segment in the performance analysis of a generic clay/shale repository.

ACKNOWLEDGEMENT

This work was supported by the Laboratory Directed Research and Development program at Sandia National Laboratories. Sandia is a multi-program laboratory operated by Sandia Corporation, a Lockheed Martin Company, for the United States Department of Energy's National Nuclear Security Administration under Contract DE-AC04-94AL85000.

REFERENCES

1. Hansen, F. D., E. L. Hardin, R. P. Rechard, G. A. Freeze, D. C. Sassani, P. V. Brady, C. M. Stone, M. J. Martinez, J. F. Holland, T. Dewers, K. N. Gaither, S. R. Sobolik, and R. T. Cygan. 2010. *Shale Disposal of U.S. High-Level Radioactive Waste*. SAND2010-2843, Sandia National Laboratories, Albuquerque, NM.
2. Edwards, H. C. 2002. *SIERRA Framework Version 3: Core Services Theory and Design*. SAND2002-3616, Sandia National Laboratories, Albuquerque, NM.
3. Notz, P.K., S.R. Subia, M.M. Hopkins, H. Moffat and D. Noble. 2007. *Aria 1.5: User Manual*. SAND2007-2734, Sandia National Laboratories, Albuquerque, NM.
4. SIERRA Solid Mechanics Team. 2009. *Adagio 4.14 User's Guide*. SAND2009-7410, Sandia National Laboratories, Albuquerque, NM.

5. DOE. 2008. *Yucca Mountain Repository Safety Analysis Report.* DOE/RW-0573, U.S. Department of Energy, Office of Civilian Radioactive Waste Management, NV.

6. Sandia National Laboratories. 2008a. *Postclosure analysis of the range of design thermal loadings.* Sandia National Laboratories. ANL-NBS-HS-000057 Rev. 00. Sandia National Laboratories, Las Vegas, NV.

7. van Genuchten, M.T. 1980. A Closed-Form Equation for Predicting the Hydraulic Conductivity of Unsaturated Soils. *Soil Science Society of America Journal*, 44, (5): 892-898.

8. Sandia National Laboratories. 2008b. *Features, Events, and Processes for the Total System Performance Assessment: Analyses.* ANL-WIS-MD-000027 REV 00. Sandia National Laboratories, Las Vegas, NV.

9. Schwartz, F. and H. Zhang. 2003. Chapter 23: Modeling Contaminant Transport. In *Fundamentals of Groundwater*. John Wiley and Sons.